Higlights

Three tephra layers were discovered in Grotta del Cavallo palaeolithic succession.

Tephra layers constrain the end of the Middle Palaeolithic at ca. 46 ka.

Uluzzian transitional complex is constrained between ca. 46 and 40 ka.

Tephrostratigraphy of Grotta del Cavallo, Southern Italy: insights on the chronology of Middle to Upper Palaeolithic transition in the Mediterranean

Giovanni Zanchetta[1,2*], Biagio Giaccio[3], Monica Bini[1,2], Lucia Sarti[4]

[1]Dipartimento di Scienze della Terra, University of Pisa, Via S. Maria 53, 56126 Pisa, Italy

[2]Istituto Nazionale di Geofisica e Vulcanologia Roma Italy.

[3]CNR - Istituto di Geologia Ambientale e Geoingegneria (IGAG), Via Salaria km 29.300, 00015 Monterotondo, Rome, Italy.

[4]Dipartimento di Scienze storiche e dei Beni culturali, University of Siena, Via Roma 56, 53100 Siena, Italy.

*Corresponding author

Abstract

The Grotta del Cavallo contains one of the most important stratification of Mousterian, Uluzzian and Final Epigravettian tecnocomplexes; its chronology is of paramount importance for understanding the timing of the transition between Middle and Upper Palaeolithic in the Mediterranean region as well as the demise of the Neanderthal and the dispersal of the first anatomically modern humans through Europe. Within the stratigraphy of the cave three different volcanic ash layers occur (layer G, Fa and C-II). They are located in the middle section of the Mousterian (layer G), in between the Mousterian and Uluzzian layers (layer Fa) and on top of the Uluzzian horizons (layer C-II). The three tephra layers were chemically fingerprinted and correlated to well-known and precisely dated widespread Late Pleistocene tephra markers. Specifically, layer G, Fa and C-II were correlated to the X-6 (108.7 ± 0.9 ka), Y-6 (45.5 ± 1.0 ka) and Campanian Ignimbrite (39.85 ± 0.14 ka), respectively. These findings provide robust chronological points allowing to conclude that: (i) the Mousterian occupation of the cave took place after the fall of the sea level following the MIS 5e high-stand; (ii) the Mousterian-Uluzzian boundary can be dated to 45.5 ± 1.0 ka and climatostratigraphically firmly placed at the transition between the Greenland Interstadial 12 (GI12)-Greenland Stadial 12 (GS12); (iii) the Uluzzian lasted for at least five millennial spanning the GS12-GI9 period and ended at beginning of the Heinrich Event 4.

Keywords: Tephrostratigraphy; Pleistocene; Paleoclimatology; Musterian; Uluzzian; Southern Italy

1. Introduction

Understanding the complex processes underlying the Palaeolithic technological change, the geographic-temporal pattern of the different cultural and biological entities, the potential role played by the Pleistocene climate change and by the variability of other components of ecosystems, are key questions in archaeology and palaeontropology (e.g. Tzedakis et al. 2007; Müller et al., 2011; Hublin, 2015;). Solving these issues requires high-resolution stratigraphic records provided with high-precision and accurate chronologies (Hublin et al., 2012; Lowe et al., 2012, 2016; d'Errico and Banks, 2015). Radiocarbon chronology represents the most powerful tool for addressing these issues, and recently has been successfully applied to the European prehistory in particular to the latest occurrence of Neanderthal, the earliest appearance of the anatomically modern human and their relation with late Middle-Early Upper Palaeolithic cultural change (e.g. Benazzi et al., 2011; Higham et al. 2014; Douka et al., 2014; Hublin, 2015). However, near or beyond ~40 ka, the higher uncertainty of the radiocarbon chronology, due to the intrinsic analytic limits – i.e., the very low content of ^{14}C and the proneness of the samples to be contaminated by younger organic material (e.g. Woods et al., 2010) – and of the radiocarbon calibration (e.g. Reimer et al., 2013; Giaccio et al. 2017a), often makes the dating of this time-interval challenging.

Palaeolithic successions of the central Mediterranean and Eastern Europe areas are often characterized by the occurrence of tephra layers being downwind the intense explosive activity of the Italian volcanoes. These layers have increasingly represented fundamental stratigraphic and chronological constrains for the archaeological investigations in these regions (e.g. Giaccio et al., 2008; Lowe et al., 2012, 2016; Aureli et al., 2015; Marra et al., 2016; Pereira et al., 2015; Villa P. et al., 2016; Villa V. et al., 2016). Specifically, the first systematic application of the tephrostratigraphy to archaeological successions revealed the inconsistence of the radiocarbon chronology of the southern and eastern Europe Middle-Upper Palaelothic (Giaccio et al., 2006) obtained with an ineffective sample decontamination procedure (Higham et al., 2009), so providing an important impulse for the subsequent improvement of the radiocarbon chronology and the reappraisal of the model and historical notions on the Middle-Upper Palaeolithic change (e.g. Douka et al., 2014; Higham et al., 2011). However, d'Errico and Banks (2015) discussed possible limitation of use tephra layer in archaeological reconstruction in particular during the Middle-Early Upper Palaeolithic changes.

In this paper we present the results of a tephrostratigraphic investigation of the Palaeolithic succession of Grotta del Cavallo, Apulia, Southern Italy (Fig. 1). This cave is one of the rare European sites documenting in a stratigraphic ordered succession a thick Mousterian sequence, with human fossils of the latest occurrence of Middle Palaeolithic (layer F) and of Early Upper Palaeolithic (Uluzzian phase, layers E-D) with associated lithic industries; thus representing an exceptional site for addressing one of the most debated subjects of the Old World prehistory (e.g. Benazzi et al., 2011; Douka et al., 2014).

2. Site description

Grotta del Cavallo (40° 9' 18.85" N, 17° 57' 37.27" E) is a well-known Palaeolithic site located along the coast of the Bay of Uluzzo, near Nardò (Apulia, Southern Italy, Fig. 1). Excavations began in the 1960's by Arturo Palma di Cesnola and are now directed by Lucia Sarti. The first stratigraphy reported by Palma di Cesnola (1963, 1964, 2001) has been confirmed in the timeline by recent excavations. The eight-meter thick succession is divided into four main chrono-cultural units (Fig. 2): the Mousterian, layers N-F; the Archaic Upper Paleolithic (Uluzzian), layers E-D; the Final Upper Paleolithic and Mesolithic, layer B; and the Neolithic, layer A. Neolithic occurrence is of minor importance, of a purely occasional nature. Layer B, referring to the Late Glacial and the transition to the Holocene, contains a sequence of the Final Upper Paleolithic which has returned, among other things, numerous objects of movable art (Martini, 2016). Below the tephra layer C, layers D-E contain an Uluzzian sequences, as confirmed by the new excavations currently in progress. There have been some discussions about the stratigraphic integrity of layer D for the supposed presence of few "Aurignacian-like" lithic artefacts (e.g. Mussi et al., 2006) and for two anomalous young radiocarbon ages at top of this archeological horizon (Banks et al., 2013). However, Ronchitelli et al. (2014) have confuted, beyond any reasonable doubt, the presumed occurrence of Aurignatian levels above the Uluzzian succession excavated in 1964. The integrity of the Uluzzian succession (layer EIII-DI, of Palma di Cesnola stratigraphy), capped by the tephra layer C, has then been definitively confirmed by later excavations conducted by L. Sarti, which also established the occurrence of Late Glacial to post-Glacial succession (layer B, Martini and Sarti, 2017) directly laying on the volcanic level C. Therefore, layers E-D confidently represent the most continuous and possibly complete succession of deposits containing the Uluzzian techo-complex.

The base of the Uluzzian level rests directly on the top surface of Mousterian layer F, a slightly shaped erosional surface. In recent excavations, layer F has been distinguished in multiple levels (from FI to FIII), with many paleosurfaces (hearths and concentrations of lithic industries and faunal remains). A few centimeters below the paleosurface FI, the excavation brought to the light the thin and discontinuous, lenticular tephra layer Fa (Fig. 2).

For the layer F, level FII, a radiocarbon measurement (47900-42100 yr cal. BP Fabbri et al., 2016; Fig. 2) was obtained, which should be understood as an indicative dating for the upper boundary of Mousterian occupation of the Grotta del Cavallo (Sarti et al., 1998-2000) and provinding a *terminus post quem* for the bottom of the Uluzzian deposit, which was in agreement with the previous Bayesian age model that dates the oldest Uluzzian to 45,000-43,000 yr cal. BP (Benazzi et al., 2011).

In the Mousterian stratigraphic sequence of approximately 4 meters thick, the tephra layer G separates the more recent series (layer F) from those older (layers H-N), which has been developed on a beach deposit attributed to MIS-5e high-stand (Sarti et al., 2012). This attribution is consistent with geomorphological evidences in southern Puglia, supported by sparse U/Th dating, which indicated that coastal deposits at the Grotta del Cavallo should be related to MIS-5e (Belluomini et al., 2002; Mastronuzzi et al., 2007; Negri et al., 2015).

A comprehensive multidisciplinary study of the entire Mousterian sequence is in progress (Sarti, in preparation) but brief annotation and specific topic can be found in Sarti et al. 1998-2000, 2002,2012; Sarti and Martini, 2005; Trenti et al., 2012; Romagnoli 2015; Romagnoli et al., 2015,2016,2017).

During the excavations three human teeth have been discovered by Palma di Cesnola, a Neanderthal lower left second deciduous molar from the Mousterian L stratum and two from the Uluzzian layer E (Palma di Cesnola and Messeri, 1967) (these considered early *sapiens*: Benazzi et al., 2011,2012), while a new Neanderthal tooth was identified during Sarti excavations in the Mousterian FIII sublayer (Fabbri et al., 2016) (Fig. 2).

3. Material and method

In order to assure an unambiguous stratigraphic position all the three samples of the tephra layers CII, Fa and G analyzed in this study were collected during the last campaign of excavation. Tephra layers were dried at room temperature and then observed and described under stereomicroscope. A fraction of the bulk samples was embedded in epoxy resin and firstly screened for quality of glass shards using scanning electron microscopy (SEM) at the Earth Sciences Department of the University of Pisa (Philips SEM 515). Then the analyses of the 3 different layers were carried out at the Istituto di Geologia Ambientale e Geoingegneria of the Italian National Research Council (IGAG-CNR) (Rome, Italy) using a Cameca SX50 electron microprobe equipped with a five wavelength dispersive spectrometer. Operating conditions were set to 15 kV accelerating voltage; 15 nA beam current; 10-15 µm beam diameter; 20 s per element counting time; Wollastonite (Si and Ca), corundum (Al), diopside (Mg), andradite (Fe), rutile (Ti), orthoclase (K), jadeite (Na), phlogopite (F), potassium chloride (Cl), barite (S), and metals (Mn) were used as standards. The Ti content was corrected for the overlap of Ti-Ka peaks. In order to evaluate the accuracy of the electron microprobe analyses, three international secondary standards (Kakanui augite and rhyolite RLS132 glasses from the United States Geological Survey) were measured prior of each analytic run. Test results are reported in Supplementary S1).

4. Results

Three tephra layers recognised along the succession (Fig. 2), show distinctive chemical compositions (Fig. 3,4,5; full analytical results are provided in Supplementary data-set S1) and different glass shards aspect (Fig. 6). Layer CII shows trachyte-phonolite composition featured by two distinct populations with SiO_2 content ranging between ~62.5-61 wt% and 60.5-59.5 and K_2O/Na_2O ratio ranging between 1.5-1.1 and >3, respectively (Fig. 3a). Layer Fa has a very distinctive peralkaline ($Na_2O + K_2O > Al_2O_3$) rhyolitic to trachytic composition, which makes it classifiable as Pantellerite (Fig. 3b). Layer G has a nearly homogenous trachytic

composition, featured by a SiO_2 content ranging between ~63 wt% and 61 wt% and by a relatively narrow variability of the K_2O/Na_2O ratio (~1.7-0.9 Fig. 3c). Both layer CII and G share compositional features of the Campanian tephra (e.g. Tomlinson et al., 2012; 2015), while the peculiar composition of layer F allows to relate it to Pantelleria Island, which is the only source of the Mediterranean pantelleritic tephra (e.g. Paterne et al., 2008)

Based on the major element composition (Fig. 3), the stratigraphic order and the chronological constraints available for the Grotta del Cavallo succession, the three tephra layers were correlated with well-known and precisely $^{40}Ar/^{39}Ar$ dated key tephra layers of the Central Mediterranean (Figs. 1,3,4,5). Layer CII perfectly matches the chemistry of the glass from Campanian Ignimbrite (CI, also known as Y-5 from marine stratigraphy, Keller et al., 1978) and reflects almost all the spectrum of chemical variability of the CI proximal units (Smith et al., 2016). Specifically, layer CII is dominated by the most evolved component of the CI magma, which fed the Plinian fallout and lower pyroclastic units, but also includes composition of the least evolved and distinctive chemical composition of the "Breccia Museo" unit (e.g. Fedele et al., 2006; Smith et al., 2016, Fig. 3b), representing the opening phase of the eruption (Fisher et al., 1993). This variability is a really diagnostic feature that makes the attribution of the layer CII to the CI unambiguous and it is particularly evident considering the compositional ranges of pre-IC and post-IC eruptions (Fig. 3a; Tomlison et al., 2012). The occurrence of CI in the Grotta del Cavallo has been previously suggested (e.g. Giaccio et al., 2006; Douka et al., 2014), but hitherto no chemical data supporting this attribution have never been reported. The CI is the major explosive eruption occurred in the Mediterranean in the last 200 ka (e.g. Barberi et al., 1978; Costa et al., 2012; Marti et al., 2015; Smith et al., 2016) and their ash dispersed eastward covering an area over ~3.7 million km^2 (Costa et al., 2012). Such a great dispersal, coupled with its precise $^{40}Ar/^{39}Ar$ age 39.85 ± 0.14 ka (95% confidence level, Giaccio et al., 2017), which consolidated the previous $^{40}Ar/^{39}Ar$ dating (De Vivo et al., 2001), make the CI a fundamental stratigraphic marker and chronological anchor point for correlating, and addressing the related issues, of many archeological and palaeoenvironmental successions at regional to extra-regional scale (e.g. Lowe et al., 2012; Giaccio et al., 2017 and references therein).

Pantelleritic layers are rare and distinctive tephra of the Mediterranean successions (e.g. Paterne et al., 2008). Keller et al. (1978) described the most widespread layer (Fig. 1), called Y-6, in some marine cores identified within the MIS 3 and dated at around 45 ka. In the marine core ODP-963A, off Pantelleria Island, Tamburrino et al. (2012) recognized explosive activity related to the Island during MIS 3, MIS 6-MIS 5 transition and MIS 6 at ca. 42.5, 127.5, 128.1, 129.1, 188.7 and 197.7 ka (ages obtained by tuning with SPECMAP, Martinson et al., 1987). Tamburrino et al. (2012) correlated the level at 42.5 ka with Y-6 of the Keller's stratigraphy. Considering the radiocarbon ages for layers D and F (Fig. 2), and the peculiar chemical composition, the Layer Fa matches the Y-6 marine marker tephra layer (Fig. 4) (Keller et al., 1978; Tamburrino et al., 2012). This Pantelleritic layer is correlated with the Green Tuff of Pantelleria volcanic island (Fig. 1) and recently precisely dated by $^{40}Ar/^{39}Ar$ method at 45.7 ± 1.0 ka (2σ; Scaillet et al., 2013) and here recalculated,

for consistency with monitor constant used for the CI $^{40}Ar/^{39}Ar$ age – i.e., AC sanidine at 1,848 Ma corresponding to FC sanidine at 28,201 Ma (Niespolo et al., 2016) – at 45.5 ± 1.0 ka (2σ).

As far as layer G is concerned, considering its chemical composition and its stratigraphic position above the coastal marine deposits related to MIS-5e high-stand and below Y-6 tephra, should be consistent with any Campanian tephra spanning the wide time interval between ~125 ka and 45 ka. There are several eruptions which have been produced by Campanian volcanoes during this interval and which may overlap in composition with layer G, among which the Y-7, C-22, X-5 and X-6 are the most widespread (e.g. Bourne et al., 2010, 2015; Wulf et al., 2012; Giaccio et al., 2012, 2017; Insinga et al., 2014; Sulpizio et al., 2010; Tomlinson et al., 2015; Leicher et al., 2016). However, when comparing altogether, the layer G appears unequivocally correlates to X-6, which in turn is clearly distinct by the other marker tephra (Fig. 5a). The peculiar composition of the X-6 is evident not only on the Total Alkali Silica diagram (TAS, Le Bas et al., 1986), but also in the alkali ratio (K_2O/Na_2O) vs CaO (Fig. 5a), which makes the attribution of layer G unambiguous (Fig. 5b).

Firstly recognized in Ionian Sea (Keller et al., 1978), the X-6 tephra has been traced in a number of marine, lacustrine and terrestrial successions (Fig. 1c). Two recent $^{40}Ar/^{39}Ar$ dating of this tephra yielded statistically indistinguishable ages of ~110-109 ka (Iorio et al., 2014: 108.9±3.6 ka, 2σ; Regattieri et al., 2017 108.7±0.9 ka, 2σ), with the most precise dating at 108.7±0.9 ka (2σ) – also recalculated for consistency – obtained from a layer occurring in the Sulmona basin (Regattieri et al., 2017).

4 Discussion

The archaeological successions are often affected by long phases of erosion and/or non-deposition and human disturbance, and thus are usually discontinuous, making their precise correlation with continuous and accurately dated palaeoclimatic archives, like marine, lake or ice cores, challenging. Figure 1 illustrates archives over central Mediterranean containing the tephra layers identified at Grotta del Cavallo. The X-6 is a well-established marker of Greenland Stadial 24, or cold event C24 (Brauer et al., 2007; Regattieri et al., 2015, 2017; Zanchetta et al., 2016). In the high resolution multiproxy record of the marine core ODP-963A (Sprovieri et al., 2012; Tamburrino et al., 2012), aligned with Greenland ice core, the Y-6 occurs at the very end of warmer Greenland Interstadial 12 (GI12) or the very beginning of Greenland Stadial 12 (GS12; Fig. 7). Finally, the CI is definitively established as a marker of the beginning of the Heinrich Event 4 (H4, e.g. Giaccio et al., 2017a and reference therein). The position of the three tephra layers in the Grotta del Cavallo succession suggests that sedimentation rate – as expected in subaerial settings – was highly variable, with some very condensed layer (e.g. layer F) and expanded one (e.g. the interval spanning the Layers M-L), as well as the possible occurrence of sedimentary hiatus, the extent and position of which are, however, not assessable on the basis of the present data. Nevertheless some relevant observations on the chronology and

climatic context of the different cultural entities – and especially for the short and apparently continuous interval between Fa/Y-6 and CII/CI layers – can be made.

In a general panorama where Mousterian successions are often poorly dated, our finding provide robust chronological markers that refine the dating of this techno-complex at Grotta del Cavallo. The succession of Mousterian occupation start after the deposition of the beach deposits correlated to MIS 5e high-stand (ca. 116-128 ka, e.g. Muhs et al. 2015), as supported by regional geomorphological studies (Mastronuzzi et al., 2007). The human occupation of the cave is well established at time of the deposition of the tephra layer G/X-6 (108.7±0.9 ka), suggesting that it happened relatively soon after the end of the marine high-stand and the subsequent sea level fall. On the other hand, the latest Mousterian occurrence are precisely marked by the deposition of the Y-6 tephra layer of ~45.5 ka, which seals the uppermost layer containing this industry and thus represents a *terminus ante quem* for the end of the Mousterian occupation in the cave. This implies that the human tooth found by Sarti excavations (1987) in the Mousterian FIII sublayer, attributed to the Neanderthal by Fabbri et al. (2016), is older than 45.5 ka (Fig. 2, 7). The previous chronological constrain for the Neanderthal tooth was based on the radiocarbon dating of the overlying layer FII, which yielded the relatively large time-slice of 47,900–42,100 cal BP (2σ; Fabbri et al., 2016; Fig. 2). Therefore, although in agreement within this radiocarbon chronology, the recognition of the Y-6 tephra substantially narrows the chronological uncertainty associated to the radiocarbon dating of the Neanderthal tooth and in general to the age of the Mousterian end (Fig. 7, 8). The radiometric age of the Y-6 tephra layer of 45.5 ± 1.0 ka, which marks the end of the Mousterian at Grotta del Cavallo, is near the lower boundary of the end of Mousterian range determined for the southern and eastern Europe at ca. 47-40 cal ka BP (Higham et al., 2014, Fig. 8).

The same Layer Fa of 45.5 ± 1.0 ka acts as a precise *terminus post quem* for the overlying archaeological levels containing Uluzzian lithic industry. On top of the Uluzzian succession there is then the layer CII, which constrains at the Grotta del Cavallo the Uluzzian succession to be older than 39.85 ± 0.14 ka.

Given the importance of the Uluzzian technocomplex in our understanding of the appearance and spread of modern humans, the presence of the CI and Y-6 at the top and at the bottom of the Uluzzian succession, respectively, along with a new suites of radiocarbon data (Benazzi et al., 2011; Fabbri et al., 2016; Douka et al., 2014), make the Grotta del Cavallo one of the better dated site for the Upper Palaeolithic complexes of Southern Europe. Specifically, due to the complexity of radiocarbon calibration at the limit of the methods and sample contaminations (e.g. Higham et al., 2009; Giaccio et al., 2017), the recognition of the couple of CI and Y-6 tephra at Grotta del Cavallo is of great importance for consolidating the site chronology and thus for contributing to better understand the processes involved in the Middle to Upper Palaeolithic modification occurred in Europe over the early-middle part of the marine isotope stage 3 (MIS 3c-d; ~58-40 ka, Railsback et al., 2015). Furthermore, the couple of tephra layers also offers the unique opportunity to physically correlate the archaeological stratigraphy with well-established palaeoclimatic records, thus allowing an

assessment of the potential link/interference between bio-cultural evolution and the abrupt climatic change, in a way completely unaffected by the chronological uncertainties inherent either tephra dating or paleoclimatic age models (Lowe, 2011; Blockley et al., 2014).

In this regard, we note that in recent works, by using an approach based on the probability distribution functions of statistically modelled radiocarbon ages, Douka et al. (2014) and Higham et al. (2014) suggested that the start of the Uluzzian at Grotta del Cavallo might be the earliest of Italy and, considering the 2σ radiocarbon distribution, being even as old as the HE5 (Fig. 8). However, because of the lack of chronological constraints for either the lowermost Uluzzian or the uppermost Mousterian layers of Grotta del Cavallo, the authors presented this results as a tentative hypothesis, susceptible to change in the light of new data. The precisely dated and climatostratigraphically well pinpointed Fa/Y-6 tephra in between the lowermost Uluzzian levels and the most recent Mousterian occurrence at Grotta del Cavallo is thus what needed to dispel this doubt. Indeed, according to the $^{40}Ar/^{39}Ar$ age of Y-6, the Grotta del Cavallo Uluzzian is undoubtedly younger than 45.5 ± 1.0 ka (Fig. 7). Furthermore, as far as the climatic context is concerned, the position of Fa/Y-6 layer in the ODP-963A proxy records (Figs. 7 and 8) places the beginning of the Uluzzian at Grotta del Cavallo close the GI12-GS12 transition, i.e., likely during the stadial phase of the GS12 (Fig. 7). This opportunity of precisely evaluating the climatic context independently of the accuracy of both Greenland and $^{40}Ar/^{39}Ar$ chronologies, as well as of their intercalibration, is a unique prerogative of the synchronization via tephra correlation; no other chronometric methods can permit the assessment of these kind of issues with the same accuracy and degree of confidence. In this context, we note that the Y-6 layer occurs as a cryptotephra in level II12 of the Middle-Upper Palaeolithic succession of Theopetra Cave, Greece (Karkanas et al., 2015). Unfortunately, as reported by some authors (Karkanas et al., 2015) the stratigraphic integrity of this archaeological level, attributed to the Upper Paleolithic, is compromised by secondary erosional-depositional processes, since the very few diagnostic Upper Paleolithic artifacts found in this layer seem to be mixed with both older and younger archaeological materiel from the Middle Palaeolithic and Mesolithic layers. However, although the stratigraphic setting of the Theopetra Cave does not allow a precise assessment of the ethno-stratigraphic position of the Y-6 layer, the recognition of this tephra in Greece demonstrates the notable potential of the Y-6 as a super-regional marker for archaeological issues.

As far as the end of the Uluzzian is concerned, in Klissoura Cave succession, Greece (Fig. 1), Lowe et al. (2012) found CI glass shards up to the base of the layer IV, containing Aurignacian industry, topping layer V, which contains Uluzzian industry. Similarly, in the Grotta di Castelcivita, southern Italy (Fig. 1), the CI is on the top of the Proto-Aurgnacian layers (Giaccio et al., 2008; Smith et al., 2016), which in turn caps Uluzzian horizons (Gambassini, 1997). Finally, at Serino, southern Italy (Fig. 1), the CI seals an open-air Proto-Aurignacian occupation (Accorsi et al., 1979; Giaccio et al., 2006), though at this open-site there is no archaeological stratification and evidence of Uluzzian industry. Therefore, as already discussed in recent studies (e.g. Douka et al., 2014; Giaccio et al., 2017a) and confirmed by our data, CI eruption or ~40 ka can be considered the

uppermost chronological boundary for the Uluzzian. It is interesting to note that in Mediterranean records the HE4, the beginning of which is marked by the CI tephra, is associated to particularly harsh climatic conditions (Fig. 7; e.g. Fedele et al., 2003; 2008; Müller et al., 2011).

Summarising, the Grotta del Cavallo tephrostratigraphic data suggest that Uluzzian developed/appeared between the end of the relatively long a mild interstadial GI12 and the first centuries of the HE4 events (Fig. 7,8). This period is featured by the rapid alternation of three stadials (GS12, GS11 and GS10) and interstadials (GI11, GI10 and GI9) as well as comprises the first 3-4 centuries of the HE4 (Fig. 7, 8). This would suggest a high capability of adaptation of the Uluzzian Palaeolithic communities to cope the unpredictable and highly variable environmental-climatic conditions of this period, which, however, seems to cease abruptly within firsts centuries of HE4, marked by the deposition of the CI tephra. We might thus suggest that the harsh, cold and arid climatic conditions of HE4, likely exacerbated by the effects of the CI super-eruption, possibly exceeded the environmental-ecological threshold of the Uluzzian adaptability (e.g. Fedele et al., 2003; 2008; Giaccio et al., 2017a).

5 Concluding remarks

Tephrostratigraphy of Grotta del Cavallo gives fresh and important insights on the chronology of the Mousterian of Southern Italy. The recognition of the X-6 tephra (~109 ka) indicates that at Grotta del Cavallo Mousterian occupation established shortly after the fall of the sea level of the MIS 5e high-stand. Mousterian occupation seems to be lasted, though with possible discontinuity, until to the deposition of the Fa/Y-6 layer dated to 45.5 ± 1.0 ka. Uluzzian techno-complex started just after the deposition Fa/Y-6 tephra layer (~45.5 ka), which, considering its climatostratigraphic position, represents a fundamental stratigraphic marker for anchoring the beginning of the Uluzzian in southern Italy at the GI12-GS12 transition. The presence of the CI (39.85 ± 0.14 ka) at Grotta del Cavallo is definitively demonstrated in this work. Together, the Y-6 and CI tephra layers precisely constrain the Uluzzian techno-complexes between ~45.5 ka and ~39.85 ka or between the GI12-GS12 transition and the early stage of GS9-HE4. Considering its dispersion (Fig. 1b), the Y-6 layer together with the already well-established marker of the CI can form a pivotal couple of tephra/cryptotephra for evaluating the age, the temporal relationship, the geographical pattern and the climatic context of the most recent Mousterian occurrences as well as of the start and the end of the Early Upper Palaeolithic, in a wide area of the southern Italy and Balkan regions. The assessment of these temporal-spatial issues is fundamental for understanding the dynamics and the ecological-anthropological factors underlying the complex mosaic of the cultural and biological modifications occurred in Europe over the early-middle MIS 3 period.

Finally, from a broader methodological perspective, our study consolidates the relevance of the tephrostratigraphy as a key, indispensable chronological-correlation tool for assessing and/or refining the

chronology of archaeological successions near or beyond the limit of the radiocarbon dating method. Certainly, by considering the conspicuous activity of the Quaternary explosive volcanisms in Mediterranean area, the recent development of cryptotephra studies and the improvement of the $^{40}Ar/^{39}Ar$ dating method, the potential of tephrostraigraphy of this region has still a wide room of enhancing.

Acknowledgements

Part of this analytical work benefit from University of Pisa financial support (Fondi di Ateneo). M.B. B.G., and G.Z contributed to the acquisition, elaboration and discussion of the geoarcheological and geochemical data. L.S. provided the general stratigraphic and archaeological framework of the site based on data from new excavations (financed by University of Siena and MIUR project-PRIN 2010-2011) and previous studies. All the authors conceived and designed the manuscript with the general conclusions. The authors thanks F. Martini and D. Lo Vetro for their valuable discussion. We also thanks two anonymous reviewers for the valuable comments, which improved the quality of the manuscript.

References

Accorsi, C.A., Aiello E., Bartolini, C., Castelletti L., Rodolfi G., Ronchitelli A., 1979.Il giacimento paleolitico di Serino (Avellino): stratigrafia, ambienti e paletnologia. Atti Soc. Tosc. Sc. Nat., Mem. Ser. A, 86, 435-487.

Aureli, D., Contardi, A., Giaccio, B., Jicha, B., Lemorini, C., Madonna, S., Magri, D., Marano, F., Milli, S., Modesti, V., Palombo, M.R., Rocca, R., 2015. Palaeoloxodon and human interaction: Depositional setting, chronology and archaeology at the Middle Pleistocene Ficoncella site (Tarquinia, Italy). PLoS ONE, 10 (4), e0124498.

Banks, W.E., d'Errico, F., Zilhão, J., 2013. Human-climate interaction during the Early Upper Palaeolithic: testing the hypothesis of an adaptive shift between the Proto-Aurignacian and the Early Aurignacian. J. Hum. Evol. 64, 39-55.

Barberi, F., Innocenti, F., Lirer, L., Munno, R., Pescatore, T., Santacroce, R., 1978. The Campanian Ignimbrite: a major prehistoric eruption in the Neapolitan area, Italy. Bull. Volcanol. 41, 10–31.

Belluomini, G., Caldara, M., Casini, C., Cerasoli, M., Manfra L., Mastronuzzi, G., Palmentola, G., Sanso, P. Tuccimei, P., Vesica, P.L., 2002. The oge of Late Pleistocene shorelines and tectonic activity of Taranto area, Southern Italy. Quat. Sc. Rev. 21, 525-547.

Benazzi, S., Douka, K., Fornai, C., Bauer, CC., Kullmer, O., Svoboda, J., Pap, I., Mallegni, F., Bayle, P., Coquerelle, M., Condemi, S., Ronchitelli, A., Harvati, K., Weber, G.W., 2011. Early dispersal of modern humans in Europe and implications for Neanderthal behavior. Nature 479, 525-528.

Benazzi, S., Fornai, C., Buti, L., Toussaint, M., Mallegni, F., Ricci, S., Gruppioni, G., Weber, G., Condemi, S., Ronchitelli, A. 2012. Cervical and crown outline analysis of Neanderthal worn and modern human lower second deciduous molars. Am. J. Physic. Anthropol., 149, 537-546.

Blockley, S., Rasmussen, S.O., Harding, P., Brauer, A., Davies, S., Hardiman, M., Lane, C., Macleod, A., Matthews, I., Wulf, S., Zanchetta, G. 2014. Tephrochronology and the extended INTIMATE (Integration of ice-core, marine and terrestrial records) event stratigraphy 8-110 ka B2K. Quat. Sc. Rev. 106, 88-100.

Bourne, A.J., Albert, P.G., Matthews, I.P., Trincardi, F., Wulf, S., Asioli, A., Blockley, S.P., Keller, J., Lowe, J.J., 2015. Tephrochronology of core PRAD 1-2 in the Adriatic Sea: insights into Italian explosive volcanism for the period 200-80 ka. Quat. Sc. Rev. 16, 28-43.

Bourne A.J., Lowe, J.J., Trincardi, F., Asioli A., Blockley S.P.E., Wulf S., Matthews I.P., Piva A., Vigliotti L. 2010. Distal tephra record for the last ca 105,000 years from core PRAD 1-2 in the central Adriatic Sea: implications for marine tephrostratigraphy. Quat. Sc. Rev., 29, 3079-3094.

Brauer, A., Allen, J.R.M., Mingram, J., Dulski, P.,Wulf, S., Huntley, B., 2007. Evidence for the last interglacial chronology and environmental change from Southern Europe. Proc. Nat. Ac. Sc. USA 104, 450–455.

Costa, A., Folch, A., Macedonio G., Giaccio, B., Isaia, R., Smith V.C., 2012. Quantifying volcanic ash dispersal and impact of the Campanian Ignimbrite super-eruption. Geophys. Res. Let., 39, 10.

D'Antonio, M., Arienzo, I., Mariconte, R., Mazzeo, F.C., Perugini, D., Petrelli, M., Civetta, L., Corselli, C., Orsi, G., Principato, M.S., 2016. Combined Sr-Nd isotopic and geochemical fingerprinting as a tool to identify tephra layers: application to deep-sea cores from Eastern Mediterranean Sea. Chem. Geol. 443, 121-136.

d'Errico, F., Banks, W.E., 2015. Tephra studies and the reconstruction of Middle-to-Upper Paleolithic cultural trajectories. Quat. Sc. Rev. 118, 182-193.

De Vivo, B., Rolandi, G., Gans, P.B., Calvert, A., Bohrson,W.A., Spera, F.J., Belkin, H.E., 2001. Newconstraints on the pyroclastic eruptive history of the Campanian volcanic Plain (Italy). Mineral. Petrogr. 73, 47–65.

Donato, P., Albert, P.G., Crocitti, M., De Rosa, R., Menzies, M.A., 2016. Tephra layers along the southern Tyrrhenian coast of Italy: Links to the X-5 and X-6 using volcanic glass geochemistry. J. Volcanol. Geotherm. Res. 317, 30-41.

Douka, K., Jacobs Z., Lane, C., Grün, R., Farr, L., Hunt C., Inglis, R.H., Reynolds T., Alberth,P., Aubert, M., Cullen, V., Hill, E., Kinsley, L., Roberts, R.G., Tomlinson, E.L., Wulf, S.,Barker G., 2014. The chronostratigraphy of the Haua Fteah cave (Cyrenaica, northeast Libya). J. Hum. Evol. 66, 39-63.

Fabbri, P.F., Panetta, D., Sarti, L., Martini, F., Salvadori, PA., Caramella, D., Fedi, M., Benazzi, S., 2016. Middle Palaeolithic human deciduous incisor from Grotta del Cavallo, Italy. Am. J. Phys. Anthropol., 1-7, DOI 10.1002 / ajpa.23044.

Fedele, F.G., Giaccio, B., Isaia, R., Orsi, G., 2003. The Campanian Ignimbrite eruption, Heinrich Event 4, and the Paleolithic change in Europe: a high-resolution investigation. A. Robock, C., Oppenheimer (Eds.), Volcanism and the Earth's Atmosphere, Geophysical Monography, 139, Am. Geophys. Un., Washington (DC) (2003), pp. 301-325.

Fedele, F. G., Giaccio, B., Hajdas, I., 2008. Timescales and cultural process at 40,000 BP in the light of the Campanian Ignimbrite eruption, western Eurasia. J. Hum. Evol., 55, 834–857.

Fedele, L., Scarpati, C., Sparice, D., Perrotta, A., Laiena, F., 2016. A chemostratigraphic study of the Campanian Ignimbrite eruption (Campi Flegrei, Italy): insights on magma chamber withdrawal and deposit accumulation as revealed by compositionally zoned stratigraphic and facies framework. J. Volcanol. Geoth. Res., 324, 105-117.

Fisher, R.V., Orsi, G., Ort, M., Heiken, G., 1993. Mobility of large-volume pyroclastic flow-emplacement of the Campanian Ignimbrite, Italy. J. Volcanol. Geoth. Res., 56, 205–220.

Francke, A., Wagner, B, Janna, Just, J., Leicher, N., Gromig, R., Baumgarten, H., Vogel, H., Lacey, J.H., Sadori, L., Wonik, T., Leng, M.J., Zanchetta, G., Sulpizio, R., Giaccio, B. 2016. Sedimentological processes and environmental variability at Lake Ohrid (Macedonia, Albania) between 637 ka and the present. Biogeosc., 13, 1179–1196.

Gambassini, P., 1997. Il Paleolitico di Castelcivita, Culture e Ambiente. Electa Napoli, Naples.

Giaccio, B., Hajdas, I., Isaia, R., Deino, A., Nomade, S., 2017a. High-precision ^{14}C and $^{40}Ar/^{39}Ar$ dating of the Campanian Ignimbrite (Y-5) reconciles the time-scales of climatic-cultural processes at 40 ka. Sc. Reports 7:45940, DOI: 10.1038/srep45940.

Giaccio, B., Niespolo E.M., Pereira, A., Nomade, S., Renne, P.R., Albert, P.G., Arienzo, I., Regattieri, E., Wagner, B., Zanchetta, G., Gaeta, M., Galli, P., Mannella, G., Peronace, E., Sottili, G., Florindo, F., Leicher, N., Marra, F., Tomlinson, E.T., 2017b. First integrated tephrochronological record for the last ~190 kyr from the Fucino Quaternary lacustrine succession, central Italy. Quat. Sc. Rev., 158, 211-234.

Giaccio, B., Hajdas, I., Peresani, M., Fedele, F.G., Isaia, R., 2006. The Campanian Ignimbrite tephra and its relevance for the time of Middle to Upper Palaeolithic shift. In: Conard NJ, Editor. When Neanderthals and Modern Humans Met. Kerns Verlag, Tübingen, Germany. 343-375.

Giaccio, B., Isaia, R., Fedele, F.G., Di Canzio, E., Hoffecker, J., Ronchitelli, A., Sinitsyn, A.A., Anikovich, M., Lisitsyn, S.N., Popov, V.V., 2008. The Campanian Ignimbrite and Codola tephra layers: Two temporal/stratigraphic markers for the Early Upper Palaeolithic in southern Italy and eastern Europe. J. Volcanol. Geoth. Res., 177 (1), 208-226.

Giaccio, B., Nomade, N., Wulf, S., Isaia, R., Sottili, G., Cavuoto, G., Galli, P., Messina, P., Sposato, A., Sulpizio, R., Zanchetta, G. 2012. The late MIS 5 Mediterranean tephra markers: a reappraisal from peninsular Italy terrestrial records. Quat. Sc. Rev., 56, 31-45.

Higham, T., Compton, T., Stringer, C., Jacobi, R., Shapiro, B., Trinkaus, E., Chandler, B., Gröning, F., Collins, C., Hillson, S., O'Higgins, P., FitzGerald, C., Fagan, M., 2011. The earliest evidence for anatomically modern humans in northwestern Europe. Nature, 479 (7374), 521-524.

Higham, T., Brock F., Peresani, M., Broglio A., Wood R., Douka K. 2009. Problems with radiocarbon dating the middle to upper palaeolithic transition in Italy. Quat. Sc. Rev. 28, 1257-1267.

Higham, T., Douka, K., Wood, R., Ramsey, C.B., Brock, F., Basell, L., Camps, M., Arrizabalaga, A., Baena, J., Barroso-Ruíz, C., Bergman, C., Boitard, C., Boscato, P., Caparrós, M., Conard, N.J., Draily, C., Froment, A., Galván, B., Gambassini, P., Garcia-Moreno, A., Grimaldi, S., Haesaerts, P., Holt, B., Iriarte-Chiapusso, M.-J., Jelinek, A., Jordá Pardo, J.F., Maíllo-Fernández, J.-M., Marom, A., Maroto, J., Menéndez, M., Metz, L., Morin, E., Moroni, A., Negrino, F., Panagopoulou, E., Peresani, M., Pirson, S., De La Rasilla, M., Riel-Salvatore, J.,

454 Ronchitelli, A., Santamaria, D., Semal, P., Slimak, L., Soler, J., Soler, N., Villaluenga, A., Pinhasi, R., Jacobi, R.,
455 2014. The timing and spatiotemporal patterning of Neanderthal disappearance Nature, 512, 306-309.
456
457 Hublin, J.J., 2015. The modern human colonization of western Eurasia: when and where? Quat. Sc. Rev., 118,
458 194-210.
459
460 Hublin, J.J., Talamo, S., Julien, M., David, F., Connet, N., Bodu, P., Vandermeersch, B., Richards, M.P.,
461 2012.Radiocarbon dates from the Grotte du Renne and Saint-Césaire support a Neandertal origin for the
462 Châtelperronian. Proc. Nat. Ac.Sc. USA, 109, 18743-18748.
463
464 Insinga, D.D., Tamburrino, S., Lirer, F., Vezzoli, L., Barra, M., De Lange, G.J., Tiepolo, M., Vallefuoco, M.,
465 Mazzola, S., Sprovieri, M., 2014. Tephrochronology of the astronomically-tuned KC01B deep-sea core, Ionian
466 Sea: insights into the explosive activity of the Central Mediterranean area during the last 200ka.
467 Quat. Sci. Rev. 85, 63-84.
468
469 Iorio, M., Liddicoat, J., Budillon, F., et al. 2014. Combined palaeomagnetic secular variation and petrophysical
470 records to time constrain geological and hazardous events: an example from the eastern Tyrrhenian Sea over
471 the last 120 ka. Glob. Planet. Ch., 113, 91–109.
472
473 Karkanas, P., White, D., Lane, C.S., Stringer, C., Davies, W., Cullen, V.L., Smith, V.C., Ntinou, M., Tsartsidou,
474 G., Kyparissi-Apostolika, N., 2015. Tephra correlations and climatic events between the MIS6/5 transition and
475 the beginning of MIS3 in Theopetra Cave, central Greece. Quat. Sc. Rev., 118, 170-181.
476
477 Keller, J., Ryan, W.B.F., Ninkovich, D., Altherr, R., 1978. Explosive volcanic activity in the Mediterranean over
478 the past 200,000 years as recorded in deep-sea sediments. Geol. Soc. Am. Bull. 89, 591–604.
479
480 Kraml, M., 1997. Laser-^{40}Ar/^{39}Ar-Datierungen an distalen marinen Tephren des jung-quart.aren mediterranen
481 Vulkanismus (Ionisches Meer, METEOR-Fahrt 25/4). Ph.D. Thesis, Albert-Ludwigs- Universit.at Freiburg i.Br.,
482 216 pp.
483
484 Le Bas, M.J., Le Maitre, R.W., Streckeisen, A., Zanettin, B., 1986. A chemical classification of volcanic rocks
485 based on the total alkali-silica diagram, J. Petrol., 27, 745-750.
486

Leicher, N., Zanchetta, G., Sulpizio, R., Giaccio, B.,Wagner, B., Nomade, S., Francke, A., Del Carlo, P., 2016. First tephrostratigraphic results of the DEEP site record from Lake Ohrid (Macedonia and Albania). Biogeosciences 13, 2151-2178.

Martini, F., Sarti, L. 2017. Nuove ricerche nei livelli "romanelliani" di Grotta del Cavallo (Lecce): le produzioni litiche e le figurazioni mobiliari, Preistoria e Protostoria - 4 - Preistoria e Protostoria della Puglia, Atti Riun. Sc. IIPP in Puglia 2012, 87-94, Firenze.

Martinson, D.G., Pisias, N.G., Hays, J.D., et al. 1987. Age dating and the orbital theory of the ice ages - development of a high-resolution-0 to 300,000-year chronostratigraphy. Quaternary Research 27: 1–29.

Lowe, D.L., 2011. Tephrochronology and its application: a review. Quaternary Geochronology 6, 107–153.

Lowe, J., Barton, N., Blockley, S., Ramsey, C.B., Cullen, V.L., Davies, W., Gamble, C., Grant, K., Hardiman, M., Housley, R., Lane, C.S., Lee, S., Lewis, M., MacLeod, A., Menzies, M., Müller, W., Pollard, M., Price, C., Roberts, A.P., Rohling, E.J., Satow, C., Smith, V.C., Stringer, C.B., Tomlinson, E.L., White, D., Albert, P., Arienzo, I., Barker, G., Borić, D., Carandente, A., Civetta, L., Ferrier, C., Guadelli, J.-L., Karkanas, P., Koumouzelis, M., Müller, U.C., Orsi, G., Pross, J., Rosi, M., Shalamanov-Korobar, L., Sirakov, N., Tzedakis, P.C., 2012. Volcanic ash layers illuminate the resilience of Neanderthals and early modern humans to natural hazards. Proc. Nat. Ac. Sc. USA, 109, 13532-13537.

Lowe, J.J., Bronk Ramsey, C., Housley, R.A., Lane, C.S. Tomlison, E.L., RESET Team, RESET Associates 2015. The RESET project: constructing a European tephra lattice for refined synchronisation of environmental and archaeological events during the last c. 100 ka. Quat. Sc. Rev., 118, 1-17.

Marciano, R., Munno, R., Petrosino, P., Santangelo, N., Santo, A., Villa, I. 2008. Late quaternary tephra layers along the Cilento coastline (Southern Italy). J. Volcanol. Geother. Res., 177, 227–243.

Marra, F., Ceruleo, P., Jicha, B., Pandolfi, L., Petronio, C., Salari, L., Giaccio, B., Sottili, G. 2016. Chronostratigraphic constraints on Middle Pleistocene faunal assemblages and Acheulian industries from the Cretone lacustrine basin, central Italy. J. Quat. Sc., 31, 641-658.

Marti, A., Folch, A., Costa, A., Engwell, S. 2015. Reconstructing the plinian and coignimbrite sources of large volcanic eruptions: A novel approach for the Campanian Ignimbrite. Sc. Report, 6, 21220; doi: 10.1038/srep21220.

Martini, F. 2016, L'arte paleolitica e mesolitica in Italia, Millenni. Studi di archeologia preistorica, 12, Firenze.

Mastronuzzi, G., Quinif, Y., Sansò, P., Selleri, G., 2007. Middle-Late Pleistocene polycyclic evolution of a stable coastal area (southern Apulia, Italy). Geomorphology, 86, 393-408.

Muhs, D.R., Simmons, K.R., Meco, J., Porat, N., 2015. Uranium-series ages of fossil corals from Mallorca, Spain: The "Neotyrrhenian" high stand of the Mediterranean Sea revisited. Palaeogeogr., Palaeoclimatol., Palaeoecol., 438, 408–424.

Müller, U.C., Pross, J., Tzedakis, P.C., Gamble, C., Kotthoff, U., Schmiedl, G., Wulf, S., Christanis, K., 2011.The role of climate in the spread of modern humans into Europe. Quat. Sc. Rev., 30, 273-279.

Mussi, M., Gioia, P., Negrino, F., 2006. Ten small sites: the diversity of the Italian Aurignacian. In: Bar-Yosef, O., Zilhão, J. (Eds.), Toward a Definition of the Aurignacian. Trabalhos de Arqueologia 45, Lisbon, pp. 189-209.

Negri, A., Amorosi, A., Antonioli, F., Bertini, A., Florindo, F., Lurcock, P.C., Marabini, S., Mastronuzzi G., Regattieri, E., Rossi, V., Scarponi, S., Taviani, M., Zanchetta, G., Vai, G.B., 2015. A potential Global Stratotype Section and Point (GSSP) for the Tarentian Stage, Upper Pleistocene, from the Taranto area (Italy): Results and future perspectives. Quat. Inter., 383, 145-157.

Niespolo, E. M., Rutte, D., Deino, A. L., Renne, P., 2016. Intercalibration and age of the Alder Creek sanidine $^{40}Ar/^{39}Ar$ standard. Quat. Geochron., doi: 10.1016/ j.quageo.2016.09.004.

North Greenland Ice Core Project Members. 2004. High-resolution record of Northern Hemisphere climate extending into the last interglacial period. Nature, 431, 147–151.

Palma de Cesnola, A. 1963. Prima campagna di scavi nella Grotta del Cavallo presso Santa Caterina (Lecce). Riv. Sc. Preist., XVIII, 41-74.

Palma de Cesnola, A. 1964. Seconda campagna di scavi nella Grotta del Cavallo presso Santa Caterina (Lecce). Riv. Sc. Preist., XIX, 23-40.

Palma di Cesnola, A., 2001. Il Paleolitico inferiore e medio in Italia, Millenni. Studi di Archeologia Preistorica, 3, Firenze, 1-352.

Palma di Cesnola, A., Messeri M.P., 1967. Quatre dents humaines paléolithiques trouvées dans des cavernes de l'Italie Méridionale. L'Anthropologie, 71, 249-262.

Paterne, M., Guichard, F., Duplessy, J.C., Siani, G., Sulpizio, R., Labeyrie, J., 2008. A 90,000– 200,000 years marine tephra record of Italian volcanic activity in the Central Mediterranean Sea. J. Volcanol. Geother. Res., 177, 187–196.

Pereira, A., Nomade, S., Voinchet, P., Bahain, J. J., Falguères, C., Garon, H., Lefèvre, D., Raynal, J. P., Scao, V. and Piperno, M., 2015., The earliest securely dated hominin fossil in Italy and evidence of Acheulian occupation during glacial MIS 16 at Notarchirico (Venosa, Basilicata, Italy). J. Quat. Sc., 30, 639–650.

Railsback, R.B., Gibbard, P.L., Head, M.J., Voarintsoa, N.R.G., Toucanne, S., 2015. An optimized scheme of lettered marine isotope substages for the last 1.0 million years, and the climatostratigraphic nature of isotope stages and substages. Quat. Sc. Rev., 111, 94–106.

Regattieri, E., Giaccio, B., Nomade, S., Francke, A., Vogel, H., Drysdale, R.N., Perchiazzi, N., Wagner, B., Gemelli, M., Mazzini, I., Boschi, C., Galli, P., Peronace, E., 2017. A Last Interglacial record of environmental changes from the Sulmona Basin (central Italy). Palaeogeogr., Palaeoclimatol., Palaeoecol., 472, 51-66.

Regattieri, E., Giaccio, B., Zanchetta, G., Drysdale, R.N., Galli, P., Nomade, S., Peronace, E., Wulf, S., 2015. Hydrological variability over the Apennines during the Early Last Glacial precession minimum, as revealed by Romagnoli, F., 2015. A second life: recycling production a stable isotope record from Sulmona basin, Central Italy. J. Quat. Sc., 30, 19-31.

Reimer, P.J., Bard, E., Bayliss, A., Beck, J.W., Blackwell, P.G., Bronk Ramsey, C., Grootes, P.M., Guilderson, T.P., Haflidason, H., Hajdas, I., Hatte, C., Heaton, T.J., Homann, D.L., Hogg, A.G., Hughen, K.A., Kaiser, K.F., Kromer, B., Manning, S.W., Niu, M., Reimer, R.W., Richards, D.A., Scott, E.M., Southon, J.R., Staff, R.A., Turney, C.S.M., van der Plicht, J., 2013. IntCal13 and Marine13 radiocarbon age Calibration Curves 0-50,000 Years cal BP. Radiocarbon 55, 1869-1887.

589 Romagnoli, F., 2015. A second life: recycling production waste during the Middle Palaeolithic in layer L at
590 Grotta del Cavallo (Lecce, Southeast Italy). Quat. Int. 361, 200-211.
591
592 Romagnoli, F., Martini, F., Sarti L., 2015. Neanderthal use of *Callista chione* shells as a raw material for
593 retouched tools in southeast Italy: Analysis of Grotta del Cavallo, layer L assemblage with a new methodology.
594 J. Archaeol. Meth. Theor. 22, 1007-1037.
595
596 Romagnoli, F., Baena, J., Sarti, L., 2016. Neanderthal retouched shell tool and Quina economic and technical
597 strategies: an integrated behaviour. Quat. Int., 407, 29-44.
598
599 Romagnoli, F., Baena, J., Pardo Naranjo, A.I., Sarti, L., 2017. Evaluating the performance of the cutting edge
600 of Neanderthal shell tools: A new experimental approach. Use, mode of operation, and strength of *Callista*
601 *chione* from a behavioural, Quina perspective. Quat. Int., 427, 216-228.
602
603 Ronchitelli, A., Benazzi, S., Boscato, P., Douka, K., Moroni, A., 2014. Comments on "Human-climate
604 interaction during the Early Upper Paleolithic: Testing the hypothesis of an adaptive shift between the Proto-
605 Aurignacian and the Early Aurignacian" by William E. Banks, Francesco d'Errico, João Zilhão. J. Hum. Evol. 73,
606 107-111.
607
608 Scaillet, S., Vita-Scaillet, G., Rotolo, S.G., 2013. Millennial-scale phase relationships between ice-core and
609 Mediterranean marine records: insights from high-precision $^{40}Ar/^{39}Ar$ dating of the Green Tuff of Pantelleria,
610 Sicily Strait. Quat. Sc. Rev. 78, 141-154.
611
612 Sarti, L., Martini, F., 2005. I risultati delle nuove ricerche a Grotta del Cavallo (Nardò, Lecce), Atti Conv. "Stato
613 attuale delle scoperte speleo-archeologiche nelle grotte pugliesi", IX incontro speleologia pugliese, Lecce
614 2004, pp. 21-28.
615
616 Sarti, L., Boscato, P, Lo Monaco, M., 1998-2000. Il Musteriano finale di Grotta del cavallo nel Salento. Studio
617 preliminare. Origini 22, 45-109.
618
619 Sarti, L., Boscato, P., Martini, F., Spagnoletti, AP. 2002. Il Musteraino di Grotta del Cavallo, strati H e I. Studio
620 preliminare. Riv. Sc. Preist., LII, 21-110.
621
622 Sarti, L., Romagnoli, F., Carmignani, L., Martini, F. 2012, Grotta del Cavallo (scavi Sarti): Tradizione e
623 innovazione nella sequenza musteriana sulla base dell'indicatore litico. Atti Riun. Sc. IIPP in Puglia, in press.

Smith, V.C., Isaia, R., Engwell, S.L., Albert, P.G., 2016. Tephra dispersal during the Campanian Ignimbrite (Italy) eruption: implications for ultra-distal ash transport during the large caldera-forming eruption. Bull. Volcanol. 78, 45.

Sprovieri, M., Di Stefano, E., Incarbona, A., Salvagio Manta, D., Pelosi, N., Ribera d'Alcalà, M., Sprovieri, R., 2012. Centennial- to millennial-scale climate oscillations in the Central-Eastern Mediterranean Sea between 20,000 and 70,000 years ago: evidence from a high-resolution geochemical and micropaleontological record. Quat. Sc. Rev., 46, 126-135.

Tamburrino, S., Insinga, D.D., Sprovieri, M., Petrosino, P., Tiepolo, M., 2012. Major and trace element characterization of tephra layers offshore Pantelleria Island: insights into the last 200 ka of volcanic activity and contribution to the Mediterranean tephrochronology. J. Quat. Sc. 27, 129-140.

Tamburrino, S., Insinga, D.D., Pelosi, N., Kissel, C., Laj, C., Capotondi, L., Sprovieri, M., 2016. Tephrochronology of a ~ 70 ka-long marine record in the Marsili Basin (southern Tyrrhenian Sea). J. Volcanol. Geother. Res. 327, 23-39.

Tomlinson, E.L., Arienzo, I., Civetta, L., Wulf, S., Smith, V.C., Hardiman, M.S., Lane, C.S., Carandente, A., Orsi, G., Rosi, M., Muller, W., Menzies, M.A., 2012. Geochemistry of the Phlegraean Fields (Italy) proximal sources for major Mediterranean tephras: implications for the dispersal of Plinian and coignimbritic components of explosive eruptions. Geochim. Cosmochim. Acta 93, 102-128.

Tomlinson, E.L., Albert, P.G., Wulf, S., Brown, R.J., Smith, V.C., Keller, J., Orsi, G., Bourne, A.J., Menzies, M.A., 2014. Age and geochemistry of tephra layers from Ischia, Italy: constraints from proximal-distal correlations with Lago Grande di Monticchio. J. Volcanol. Geotherm. Res. 287, 22e39.

Tomlinson, E. L., Smith, V. C., Albert, P. G., Aydar, E., Civetta, L., Cioni, R., Çubukçu, E., Gertisser, R., Isaia, R., Menzies, M. A., Orsi, G., Rosi, M., and Zanchetta, G.. 2015. The major and trace element glass compositions of the productive Mediterranean volcanic sources: tools for correlating distal tephra layers in and around Europe, Quaternary Sci. Rev., 118, 48–66.

Trenti, F., Nannini, L., Romagnoli, F., Carmignani, L., Martini, F., Sarti, L. 2012. Grotta del Cavallo: ipotesi di mobilità dei gruppi umani musteriani sulla base dell'approvvigionamento delle materie prime. Atti Riun. Sc. IIPP in Puglia, in press.

659
660 Tzedakis, P.C., Hughen, K.A., Cacho, I., Harvati, K., 2007. Placing late Neanderthals in a climatic context.
661 Nature, 449, 206–208.
662
663 Villa, P., Soriano, S., Grün, R., Marra, F., Nomade, S., Pereira, A., et al. (2016) The Acheulian and Early Middle
664 Paleolithic in Latium (Italy): Stability and Innovation. PLoS ONE 11(8): e0160516.
665 https://doi.org/10.1371/journal.pone.0160516.
666
667 Villa, V., Pereira, A., Chaussé, C., Nomade, S., Giaccio, B., Limondin-Lozouet, N., Fusco, F., Regattieri, E.,
668 Degeai, J.-P., Robert, V., Kuzucuoglu, C., Boschian, G., Agostini, S., Aureli, D., Pagli, M., Bahain, J.J., Nicoud, E.,
669 2016. A MIS 15-MIS 12 record of environmental changes and Lower Palaeolithic occupation from Valle
670 Giumentina, central Italy. Quat. Sc. Rev. 151, 160-184.
671
672 Vogel, H., Zanchetta, G., Sulpizio, R., Wagner, B., Nowaczyk, N. 2010. A tephrostratigraphic record for the last
673 glacial-interglacial cycle from Lake Ohird, Albania and Macedonia. J. Quat. Sc., 25, 320-338.
674
675 Wood, R.E., Bronk Ramsey, C., Higham, T.F.G., 2010. Refining the ultrafiltration bone pretreatment
676 background for radiocarbon dating at ORAU. Radiocarbon 52, 600–611.
677
678 Wulf, S., Keller, J., Paterne, M., Mingram, J., Lauterbach, S., Opitz, S., Sottili, G., Giaccio, B., Albert, P.G., Satow,
679 C., Tomlinson, E.L., Viccaro, M., Brauer, A., 2012. The 100-133 ka record of Italian explosive volcanism and
680 revised tephrochronology of Lago Grande di Monticchio. Quat. Sc. Rev. 58, 104-123.
681
682 Zanchetta, G., Regattieri, E., Giaccio, B., Wagner, B., Sulpizio, R., Francke, A., Vogel, H., Sadori, L., Masi, A.,
683 Sinopoli, G., Lacey, J.H., Leng, M.J., Leicher, N. 2016. Aligning and synchronization of MIS5 proxy records from
684 Lake Ohrid (FYROM) with independently dated Mediterranean archives: implications for DEEP core
685 chronology. Biogeosciences, 13, 2757–2768.
686
687 **Figure and table captions**
688
689 **Figure 1**. Reference map and dispersal area of the investigated tephra layers with the location of Grotta del
690 Cavallo and other archaeological and palaeoclimatic records mentioned in text. **a**) Modelled dispersal area
691 of the Campanian Ignimbrite (CI) from Campi Flegrei (Costa et al., 2012; Marti et al., 2016, and reference
692 therein); **b**) Dispersal area of the Y-6 tephra, correlated to the Green Tuff of Panelleria Island. Data source:

693 SIN-SAP 98 GC101 and SIN-SAP-98 GCAP1.1: D'Antonio et al. (2016); ODP963A: Tamburrino et al. (2012);
694 MD01-2474G: Tamburrino et al. (2016); M25/4-12 and M25/4-13: Kraml (1997); Lake Ohrid, V10-68/M226-
695 60, RC9-191, RC9-190: Vogel et al. (2010); Theopetra Cave (Karkanas et al., 2015). **c**) Dispersal area of the X-
696 6 tephra. Data source: PRAD 1-2: Bourne et al. (2015); Sulmona: Regattieri et al. (2015); Fucino: Giaccio et al.
697 (2017b); Monticchio: Wulf et al. (2012); lake Ohrid (Leicher et al., 2016); KET8022 and KET8007: Paterne et
698 al. (2008); Cilento: Marciano et al. (2008), Giaccio et al. (2012) and Donato et al. (2016); M25/4-10 to M25/4-
699 10 -13: Kraml (1997).
700
701 **Figure 2**. Stratigraphy of Grotta del Cavallo succession (modified from Palma di Cesnola, 1963; 1964; 2001
702 and from Sarti et al. 2012) with two pictures showing the macroscopic aspect of the layers CII and G and the
703 SEM image of the tephra Fa. Radiocarbon chronology of the Uluzzian and Mousterian layer are from Benazzi
704 et al. (2011), Douka et al. (2014) and Fabbri et al. (2016), respectively.
705
706 **Figure 3**. Comparison between Grotta del Cavallo tephra CII and tephra from Campi Flegrei (CF)
707 caldera. **a)** total alkali versus silica classification diagram (TAS, Le Bas et al., 1986) for layer Cavallo CII, CF pre
708 Campanian Ignimbrite (CI), CF post-CI and pre-Neapolitan Yellow Tuff (NYT) and CI (data from Tomlinson et
709 al., 2012 and Smith et al., 2016). **b)** total alkali versus silica classification diagram and representative bi-plots
710 for the layer Cavallo CII compared with composition of the proximal sub-units of the CI (Smith et al., 2016).
711 UPF: Upper Pyroclastic Flow; LPF: Lower Pyroclastic Flow; BM: Breccia Museo.
712
713 **Figure 4**. Total alkali versus silica classification diagram (TAS, Le Bas et al., 1986) and representative bi-plots
714 for the Grotta del Cavallo tephra Fa compared with Y-6 tephra.
715
716 **Figure 5**. Comparison between Cavallo tephra G and tephra from Campania volcanoes chronologically
717 compatible with layer G. **a)** Total alkali versus silica classification diagram (TAS, Le Bas et al., 1986) with a
718 representative bi-plots for the Grotta del Cavallo tephra G and the most widespread Mediterranean
719 trachyte-phonolite tephra X-6, X-5, C-22 and Y-7. Total alkali versus silica classification diagram and
720 representative bi-plots for the Grotta del Cavallo tephra G and for the X-6 tephra.
721
722 **Figure 6**. SEM-EDS images of a) layer C-II, b) layer Fa; c) layer G. Note the different size of the glass shards
723 and their shape.
724
725 **Figure 7**. Tephra correlation between Grotta del Cavallo sedimentary succession with some representative
726 central Mediterranean palaeoclimatic records, containing the same tephra identified in the archaeological
727 record, and with the reference Greenland isotope profile showing the age and the climatic contest of the

different Palaeolithic occupation layers at Grotta del Cavallo. The calibrated radiocarbon chronology of Grotta del Cavallo succession (Benazzi et al., 2011; Douka et al., 2014) and the U/Th-based chronology of the MIS 5e sea level high-stand (Muhs et al., 2015) are also shown. Source: NorthGRIP ice isotope record: North Greenland Ice Core Project Members (2004); Monticchio arboreal pollen record: Brauer et al. (2007); ODP-160-963-A marine isotope record: Sprovieri et al. (2012); Sulmona lacustrine isotope record: Regattieri et al. (2017); Temaghi Philippon arboreal pollen record: Müller et al. (2011); Lake Ohrid total inorganic carbon (TIC): Francke et al. (2016), chronology according to Zanchetta et al. (2016).

Figure 8. Comparison between radiocarbon-, $^{40}Ar/^{39}Ar$- and tephro-climatostratigraphic-based chronology for the Mousterian-Uluzzian transition and of the upper boundary of the Uluzzian of Grotta del Cavallo archaeological record. While on one hand for the Uluzzian end, within the uncertainty, the three different chronologies are nearly in agreement, on the other, some differences, especially for what concern the uncertainty, can be noted between the modelled radiocarbon age for the Uluzzian start and that inferred by the $^{40}Ar/^{39}Ar$- and the climatostratigraphic-based chronologies, both in good agreement among them. Data sources: modelled radiocarbon ages of the Uluzzian start and end: Douka et al. (2014) and Hìgham et al. (2014); calibrated radiocarbon age of the Layer FII: Fabbri et al. (2016); calibrated radiocarbon and $^{40}Ar/^{39}Ar$ age of the Campanian Ignimbrite: Giaccio et al. (2017); $^{40}Ar/^{39}Ar$ age of the Green Tuff of Pantelleria: Scaillet et al. (2013); NorthGRIP ice isotope record: North Greenland Ice Core Project Members (2004); Tenaghi Philippon arboreal pollen record: Müller et al. (2011); ODP-160-963-A marine isotope record: Sprovieri et al. (2012).

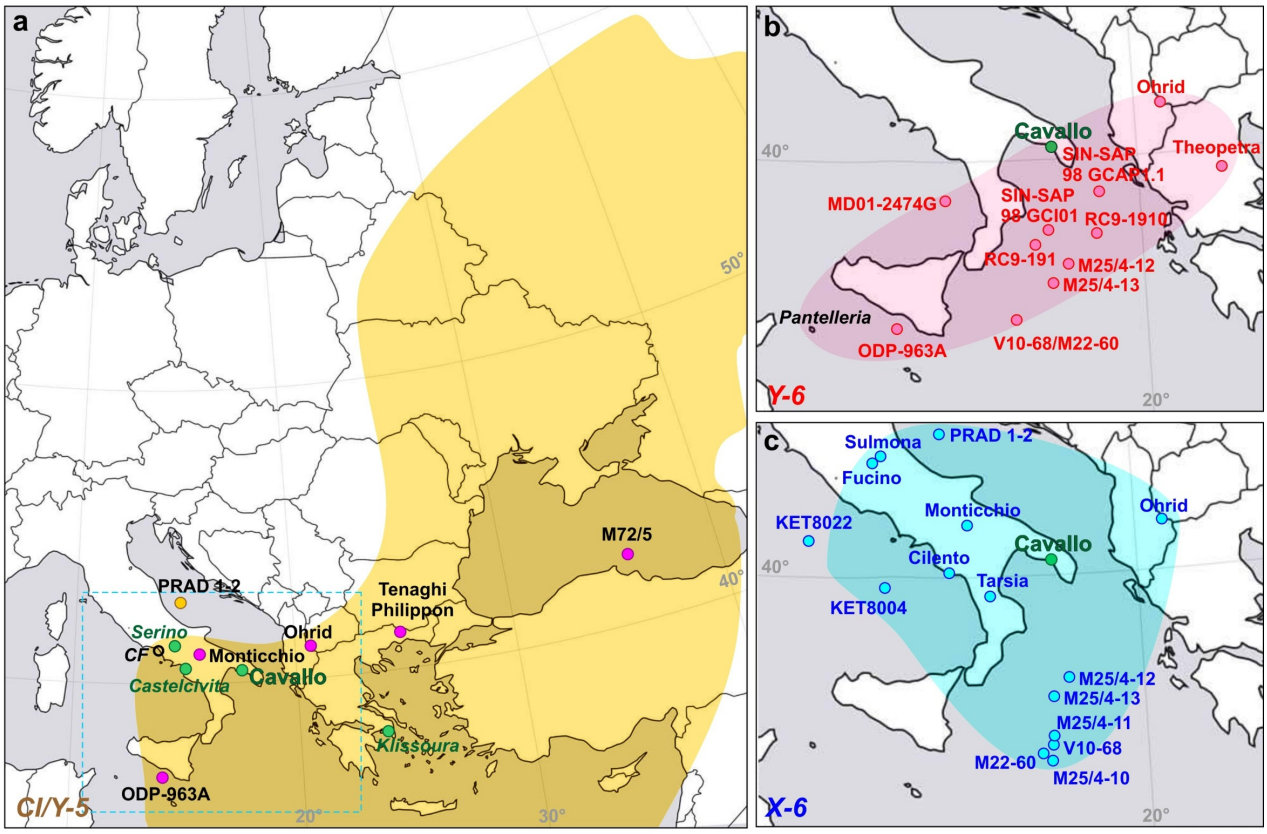

CI dispersal area (Costa et al., 2012) and other CI occuerences (dots) not included in Costa et al. (2012).

Y-6 dispersal area and related stratigrapic occurrences.

X-6 dispersal area and related stratigrapic occurrences.

Palaeolithic sites mentioned in the text.

Palaeoclimatic records mentioned in the text.

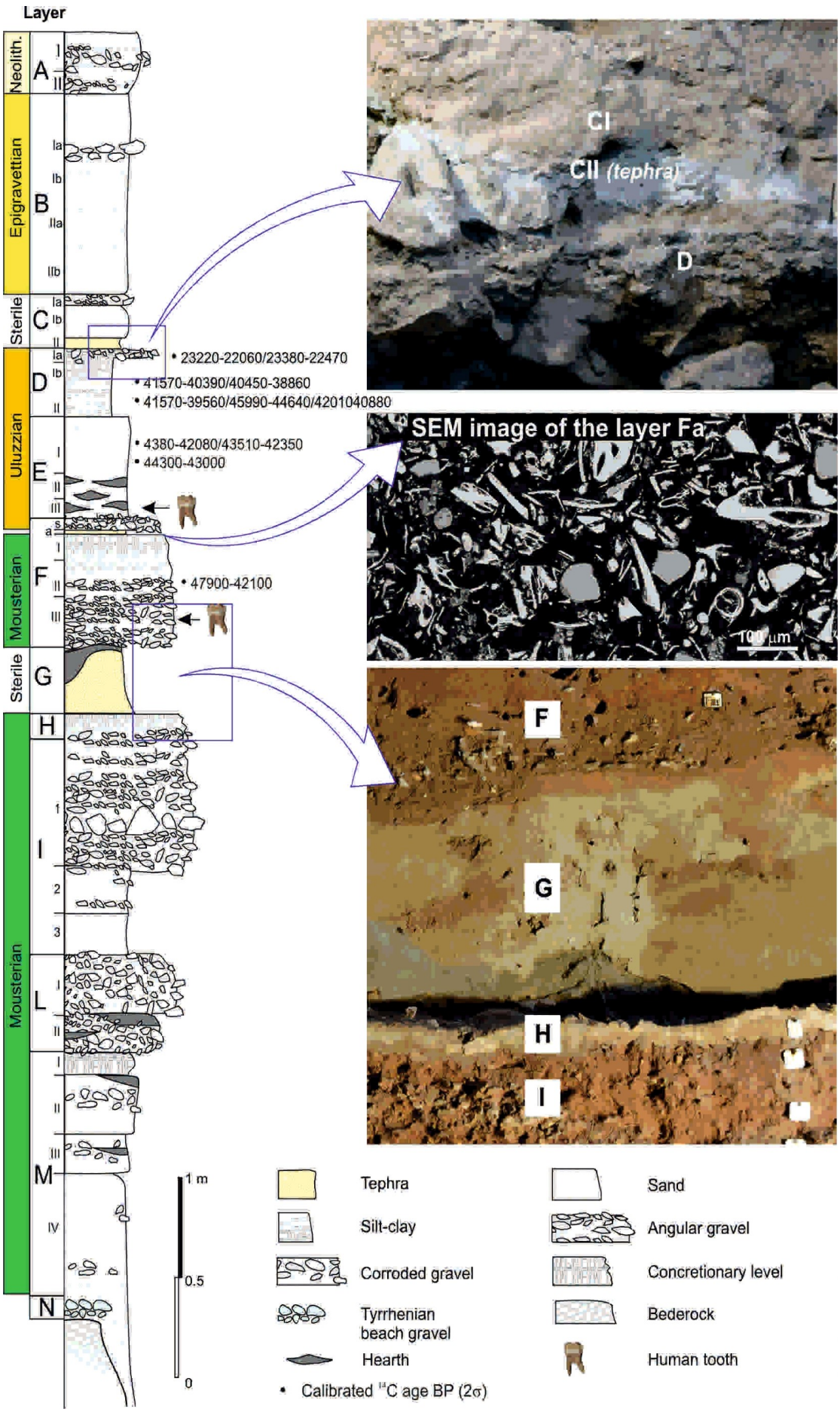
Layer
Neolith.
Epigravettian
Sterile
Uluzzian
Mousterian
Sterile
Mousterian
A
B
C
D
E
F
G
H
I
L
M
N
• 23220-22060/23380-22470
• 41570-40390/40450-38860
• 41570-39560/45990-44640/4201040880
• 4380-42080/43510-42350
• 44300-43000
• 47900-42100
CI
CII (tephra)
D
SEM image of the layer Fa
100 µm
F
G
H
I
1 m
0.5
0
Tephra
Silt-clay
Corroded gravel
Tyrrhenian beach gravel
Hearth
Calibrated 14C age BP (2σ)
Sand
Angular gravel
Concretionary level
Bederock
Human tooth

a)

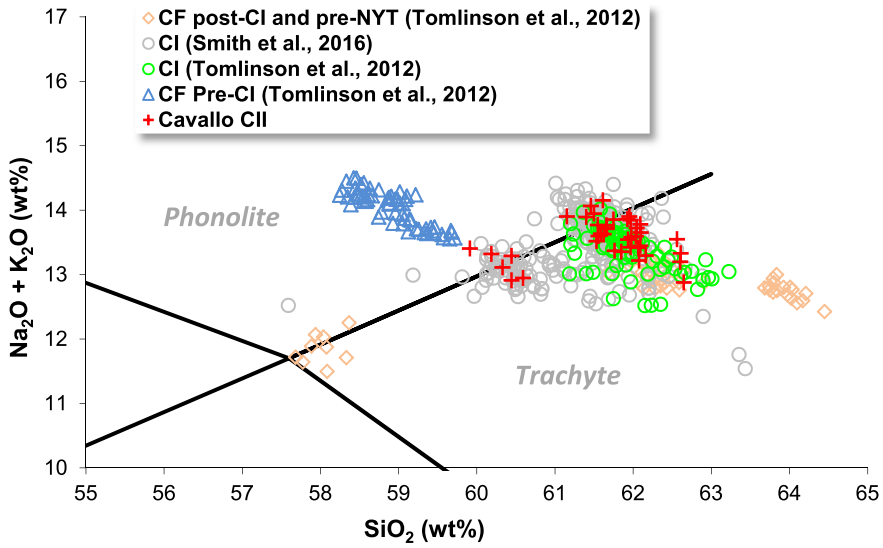
CF post-CI and pre-NYT (Tomlinson et al., 2012)
CI (Smith et al., 2016)
CI (Tomlinson et al., 2012)
CF Pre-CI (Tomlinson et al., 2012)
Cavallo CII
Phonolite
Trachyte
Na2O + K2O (wt%)
SiO2 (wt%)

b)

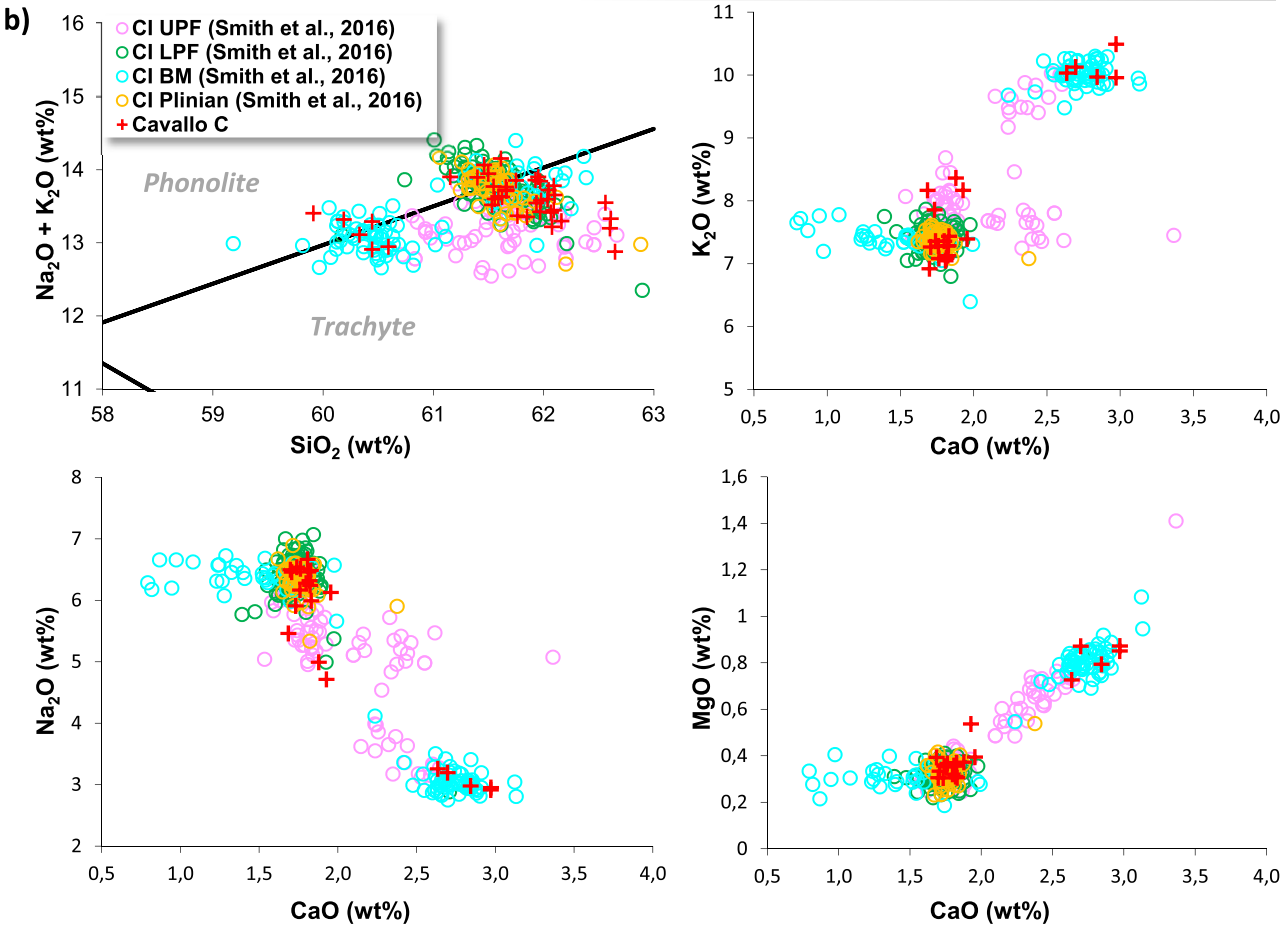
CI UPF (Smith et al., 2016)
CI LPF (Smith et al., 2016)
CI BM (Smith et al., 2016)
CI Plinian (Smith et al., 2016)
Cavallo C
Phonolite
Trachyte
Na2O + K2O (wt%)
SiO2 (wt%)
K2O (wt%)
CaO (wt%)
Na2O (wt%)
CaO (wt%)
MgO (wt%)
CaO (wt%)

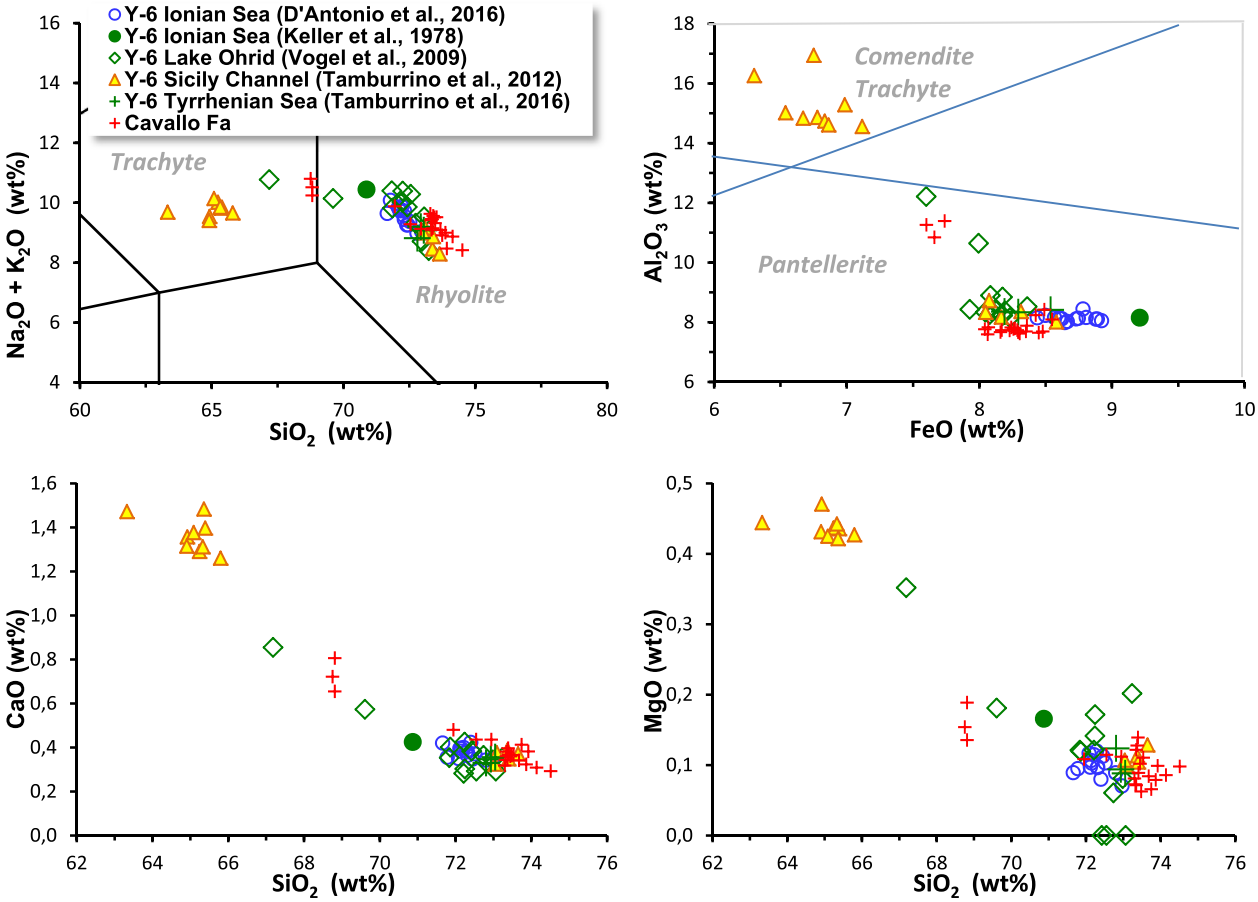
Y-6 Ionian Sea (D'Antonio et al., 2016)
Y-6 Ionian Sea (Keller et al., 1978)
Y-6 Lake Ohrid (Vogel et al., 2009)
Y-6 Sicily Channel (Tamburrino et al., 2012)
Y-6 Tyrrhenian Sea (Tamburrino et al., 2016)
Cavallo Fa
Trachyte
Rhyolite
Na2O + K2O (wt%)
SiO2 (wt%)
Comendite
Trachyte
Pantellerite
Al2O3 (wt%)
FeO (wt%)
CaO (wt%)
SiO2 (wt%)
MgO (wt%)
SiO2 (wt%)

a) *Cavallo G vs Y-7, C-22, X-5 and X-6*

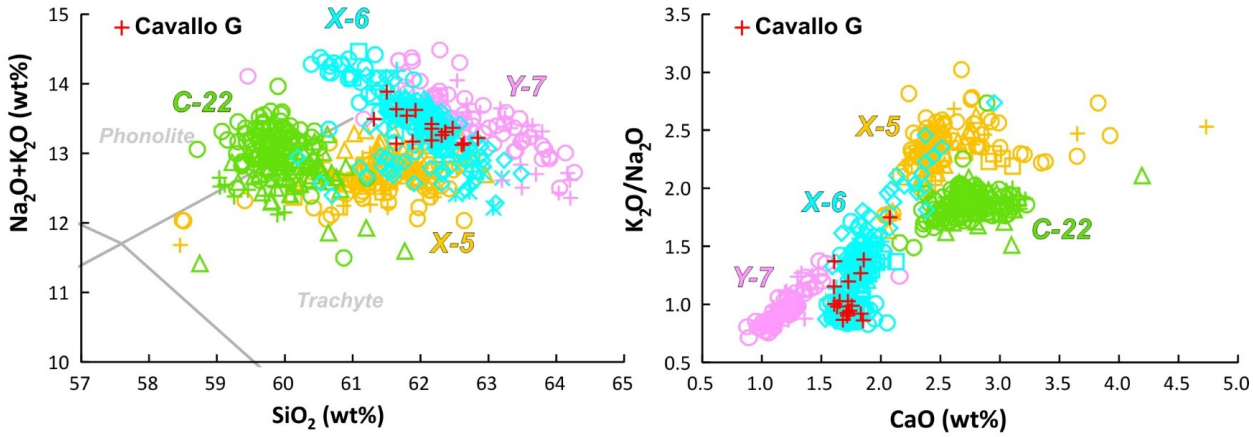

X-6
- Cilento coasts (Giaccio et al., 2012; Donato et al., 2016)
- Tyrrhenian Sea (t1; Iorio et al., 2014)
- Monticchio (TM-27; Wulf et al., 2012)
- Adriatic (PRAD2812; Bourne et al., 2015)
- Fucino (TF-13; Giaccio et al., 2017)
- Sulmona (POP4; Regattieri et al., 2015)
- Ionian Sea (I-9; Insinga et al., 2014))

X-5
- Fucino (TF-12, Giaccio et al., 2017)
- Sulmona (POP3, Giaccio et al., 2012)
- Monticchio (TM-25; Wulf et a., 2012)
- Cilento coasts (Giaccio et al., 2012)

C-22
- Adriatic Sea (PRAD2517, Bourne et al., 2010)
- Sulmona (POP1, Giaccio et al., 2012)
- Fucino (TF-10, Giaccio et al., 2017)

Y-7
- Monte Epomeo Green Tuff (Tomlinson et al., 2014)
- Adriatic Sea (PRAD 1870, Bourne et al., 2010)
- Fuciono (TF-7, Giaccio et al., 2017)

b) *Cavallo G vs X-6*

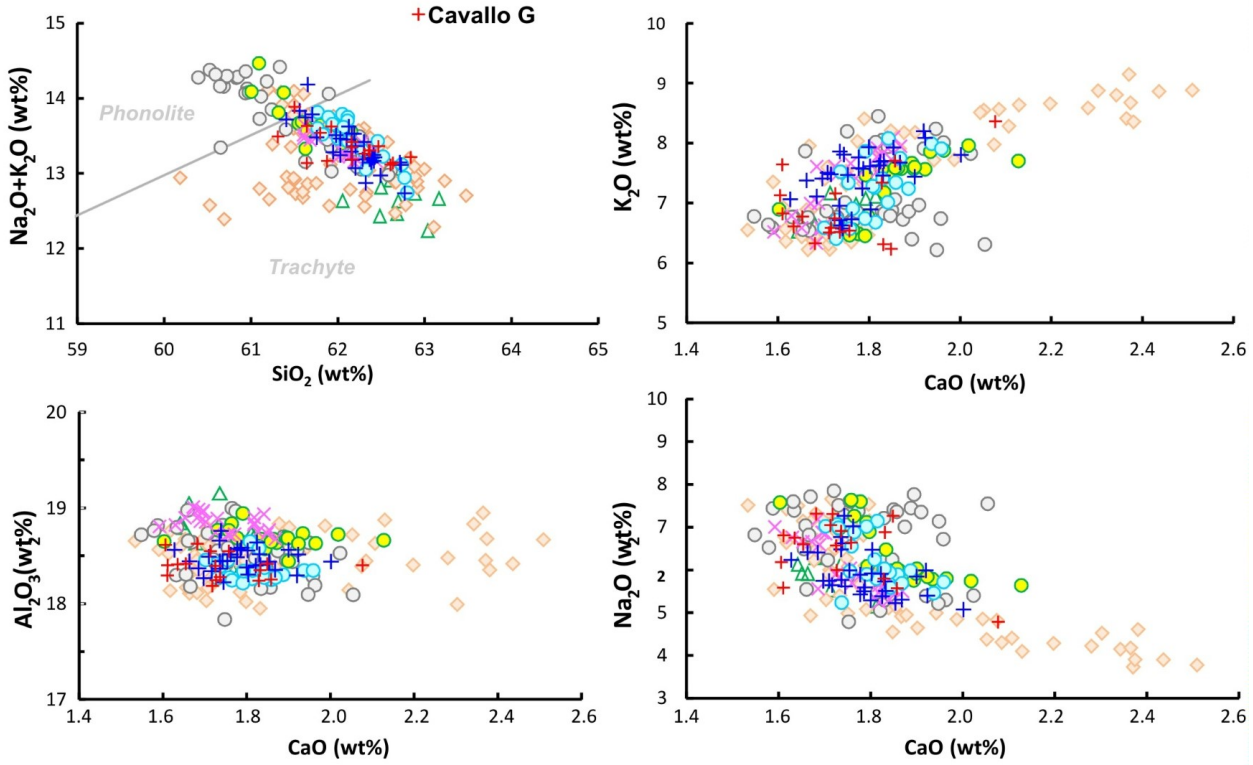

Cavallo G

X-6
- Ionian Sea (I-9; Insinga et al., 2014)
- Cilento (Giaccio et al., 2012; Donato et al., 2016)
- Tyrrhenian Sea (t1; Iorio et al., 2014)
- Monticchio (TM-27; Wulf et al., 2012)
- Adriatic (PRAD2812; Bourne et al., 2015)
- Fucino (TF-13; Giaccio et al., 2017)
- Sulmona (POP4; Giaccio et al., 2012)

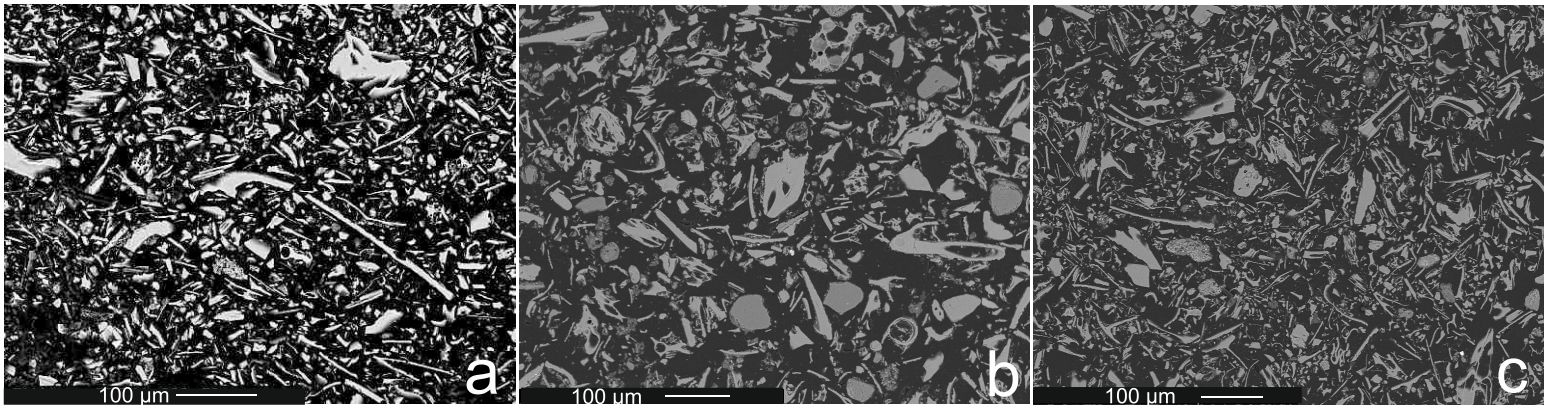
100 µm
a
100 µm
b
100 µm
c

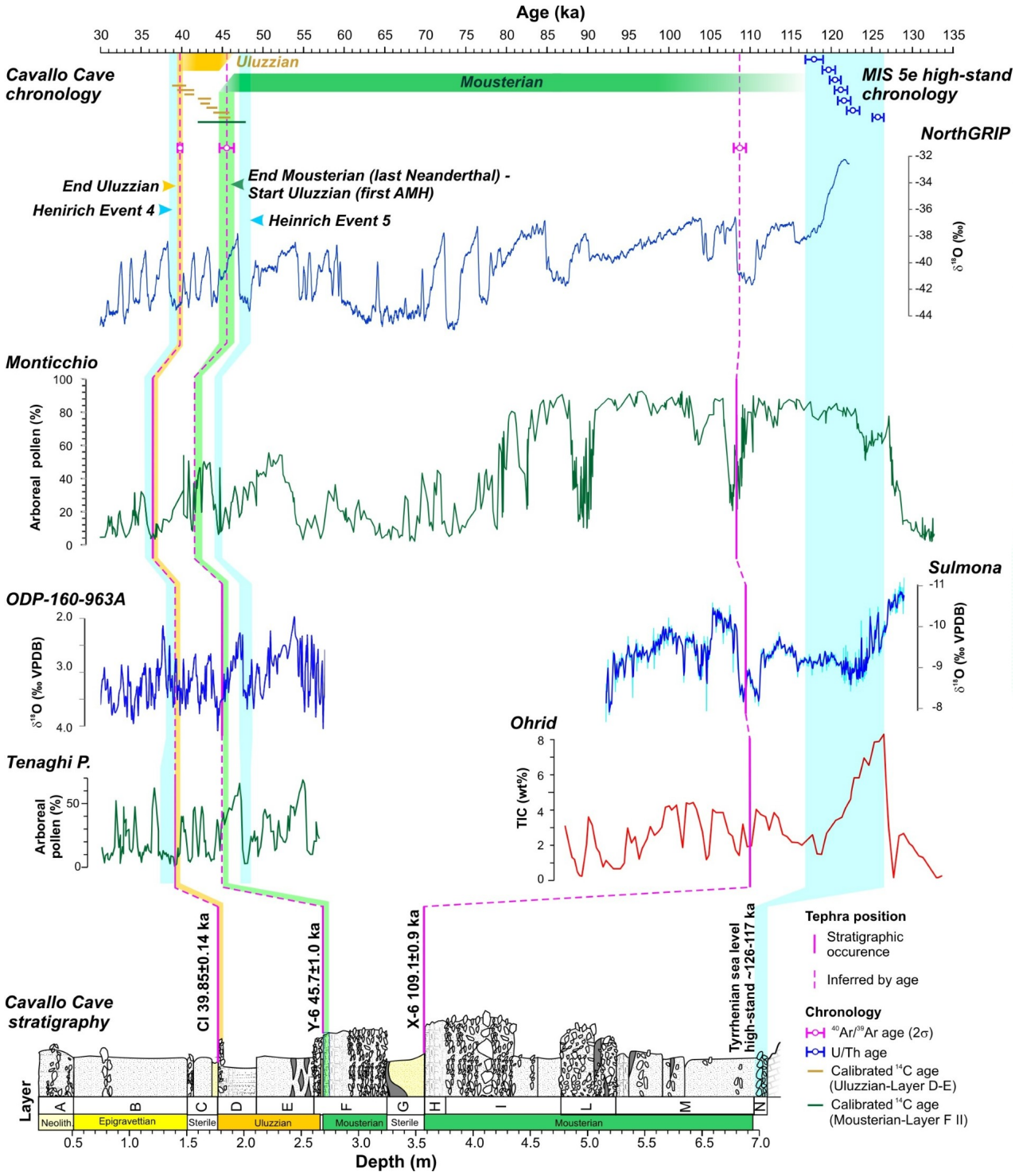
Age (ka)
Cavallo Cave chronology
Uluzzian
Mousterian
MIS 5e high-stand chronology
NorthGRIP
End Uluzzian
Henirich Event 4
End Mousterian (last Neanderthal) - Start Uluzzian (first AMH)
Heinrich Event 5
δ18O (‰)
Monticchio
Arboreal pollen (%)
Sulmona
ODP-160-963A
δ18O (‰ VPDB)
Ohrid
TIC (wt%)
Tenaghi P.
Arboreal pollen (%)
Cavallo Cave stratigraphy
CI 39.85±0.14 ka
Y-6 45.7±1.0 ka
X-6 109.1±0.9 ka
Tyrrhenian sea level high-stand ~126-117 ka
Layer
A B C D E F G H I L M N
Neolith. Epigravettian Sterile Uluzzian Mousterian Sterile Mousterian
Depth (m)
Tephra position
Stratigraphic occurence
Inferred by age
Chronology
40Ar/39Ar age (2σ)
U/Th age
Calibrated 14C age (Uluzzian-Layer D-E)
Calibrated 14C age (Mousterian-Layer F II)

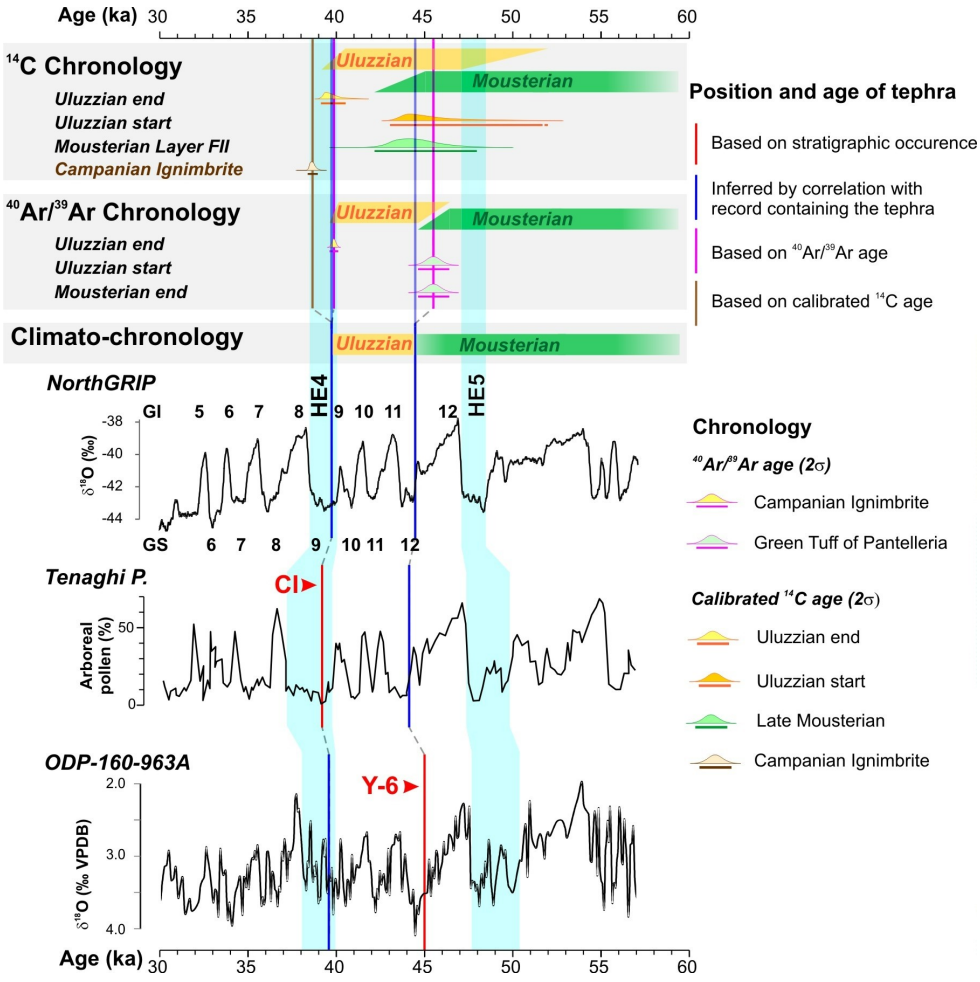
Age (ka) 30 35 40 45 50 55 60
14C Chronology
Uluzzian
Mousterian
Uluzzian end
Uluzzian start
Mousterian Layer FII
Campanian Ignimbrite
40Ar/39Ar Chronology
Uluzzian
Mousterian
Uluzzian end
Uluzzian start
Mousterian end
Climato-chronology
Uluzzian
Mousterian
NorthGRIP
HE4
HE5
GI 5 6 7 8 9 10 11 12
GS 6 7 8 9 10 11 12
δ18O (‰) -38 -40 -42 -44
Tenaghi P.
CI
Arboreal pollen (%) 50 0
ODP-160-963A
Y-6
δ18O (‰ VPDB) 2.0 3.0 4.0
Age (ka) 30 35 40 45 50 55 60
Position and age of tephra
Based on stratigraphic occurence
Inferred by correlation with record containing the tephra
Based on 40Ar/39Ar age
Based on calibrated 14C age
Chronology
40Ar/89Ar age (2σ)
Campanian Ignimbrite
Green Tuff of Pantelleria
Calibrated 14C age (2σ)
Uluzzian end
Uluzzian start
Late Mousterian
Campanian Ignimbrite